Hindawi
Advances in Civil Engineering
Volume 2019, Article ID 6568208, 13 pages
https://doi.org/10.1155/2019/6568208

Research Article

Factors Affecting the Swelling-Compression Characteristics of Clays in Yichang, China

Changxi Huang, Xinghua Wang, Hao Zhou, and Yan Liang

School of Civil Engineering, Central South University, Changsha 410075, China

Correspondence should be addressed to Xinghua Wang; xhwang@mail.csu.edu.cn

Received 16 November 2018; Accepted 13 January 2019; Published 3 February 2019

Academic Editor: Salvatore Grasso

Expansive soil has been studied for eighty decades because it is prone to cause geotechnical engineering accidents. The results of the moisture content effects on the expansive pressure were not consistent in the literatures. In this paper, swelling deformation and pressure tests were conducted to clarify the effects of the initial water content on the swelling properties. The relation of expansive stress and initial moisture content was accurately described with a Gaussian distribution, unlike in the previously published studies. These results could be explained by the change in the microstructure with diverse moisture contents. In addition, dry density and vertical stress influences on expansive properties were analysed. With an increase in the vertical loading, the soil samples first expanded, and then the samples with a lower dry density collapsed; however, the samples with a higher dry density did not collapse, even under a considerable vertical loading. Furthermore, the relation between stress path and expansive pressure was examined. It was observed that the swelling pressures obtained from the constant volume tests were greater than the results from the swell under load tests. The relationship between the swelling pressure and swelling strain was also analysed.

1. Introduction

Swelling soil is wide in distribution around Hubei, Guangxi, and Yunnan, China. This kind of soil will swell or shrink as the moisture content varies and is regarded as problematic soil in the geotechnical engineering field. Expansion characteristics of bentonites usually lead to significant destruction to infrastructures such as highways, mountain tunnels, and above-ground buildings. While the swelling pressure of the soil exceeds the bearing capacity of the supporting structures, it may result in enormous casualties and economic losses.

The swelling mechanisms have been studied based on diffuse double layer theory (e.g., Sridharan and Jayadeva [1] and Tripathy et al. [2]). Bharat et al. [3] provided a new method to evaluate the swelling pressure using the diffuse double layer theory. Schanz et al. [4] figured out the swelling pressure for different dry densities by new equations on the basis of diffuse double layer theory. The suction effect on expansive properties has been analysed (Wray et al. [5]; Adem and Vanapalli [6]; and Lin and Cerato [7]). The relation of expansive stress and suction has been demonstrated by Agus et al. [8]. Wang et al. [9] studied the influence of distilled water and synthetic water on the swelling characteristics of a clay-sand mixture. Chen et al. [10] clarified the different NaCl concentration and vertical pressure effects on swelling feature of compacted clay. Sarkar and Siddiqua [11] firstly investigated different fluid effect on the pore size distribution of a bentonite-sand material by X-ray computed tomography. Lin and Cerato [7] studied the microscale properties of expansive soils, which included suction, pH, surface conductance, and montmorillonite content. Saba et al. [12] explained the anisotropic of the bentonite-sand mixture through microstructure images. Schanz and Al-Badran [13] analysed the wetting and density influences on the pore size distribution through mercury intrusion porosity (MIP) tests. Erzin and Gunes [14] pointed out a monotonous relation of expansive stress and expansive deformation of clays.

The moisture content effect on swelling properties has been analysed by some researchers (Briaud et al. [15] and

Overton et al. [16]). Kaufhold et al. [17] conducted experiments to explain the relations between dry density and swelling pressure for different bentonites. Sivakumar et al. [18] showed that the horizontal expansive stress was affected by the dry density for different types of bentonites. Villar and Lloret [19] noted expansive deformation reduced as the initial moisture content increased under a same dry density. Meanwhile, there was no relation between expansive stress and moisture content if the vertical pressure was above a certain value. Jayalath et al. [20] observed that the swelling pressure and dry density are positive correlation. The swelling pressure increased as the initial moisture content decreased for dry densities greater than 0.125 kN/m^3.

In general, the influence of the moisture content on expansion behaviour of expansive soil was not clear. Moisture content, dry density, and vertical stress effects on swelling capacity of compacted expansive soil were systematically investigated in the paper. Some of the observed results were different from the previously published results; a combination of microstructure and expansion strain energy was used to discuss these results.

2. Testing Soil and Program

2.1. Experimental Soil. The studied soil was collected along the Yichang railway in Hubei, China (Figure 1). After the free swelling test, the free swelling strain was 41.17%, which classified this soil as weakly expansive. The liquid limit of the soil was 53.18%, the plastic limit was 24.45%, and the specific gravity was 2.477. The soil was located above line A in the plastic chart (Figure 2). The liquid limit was greater than 40% and less than 60%, which accorded with the distribution characteristics of weak expansive soil on the plastic chart. The unit mass of the solids in the soil was 0.156 kN/m^3, the natural water content was 27.3%, and void ratio was 0.588. The grain size distribution of the soil is shown in Figure 3. The mineral composition was analysed by X-ray diffraction technique. Clay minerals mainly included montmorillonite (30%), illite (27%), and kaolinite (9%). And nonclay minerals consisted of quartz (15%), feldspar (6%), and calcite (13%). The values in parentheses were mineral contents.

Based on the modified Proctor compaction method, the maximum dry density and the optimum moisture content were determined. Soil collected from field site was dried in the oven. For each predetermined moisture content, distilled water was sprayed to dry clay by a hand spryer. Then, wetting soil was put in a plastic bag and then placed in a sealed glass pot for 48 hours to achieve moisture homogenization. Next, the soil was poured into the container five times; each time weighed 1 kg. A hammer with 4.5 kg falling from 45.7 cm hit 56 times on the soil, and then the designed compaction effort (2.682×10^6 N/m^2) was attained. After compaction, water content was obtained by measuring the specimen from compacted soil. As a result, the maximum dry density and the optimum moisture content were 0.197 kN/m^3 and 16.47%, respectively.

Figure 1: Site of the sample collected.

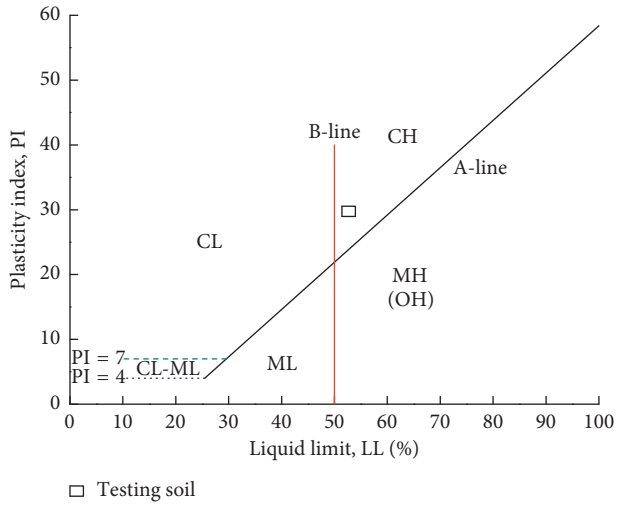

Figure 2: Plasticity chart.

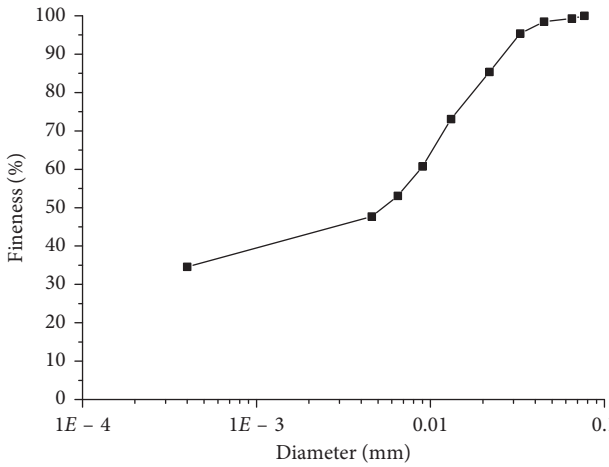

Figure 3: Granulometry of testing soil.

2.2. Sample Producing. The soil was collected from the field site and dried by the oven. Then, large pieces of the clay were squashed to particles and a 2 mm sieve was used to remove

larger clay blocks. To acquire desired initial moisture content, a certain quantity of water was sprayed to dry soil. Meanwhile, dry soil and water were mixed thoroughly to make a uniform testing soil. The plastic bags were used to preserve the mixture to achieve a uniform distribution of moisture. A certain amount of mixture was compacted in a specially constructed mould to produce a sample. The size of the sample was 76 mm in diameter and 20 mm in height. Then, the compacted specimen (Figure 4) was carefully transferred into another oedometer ring to minimize the possible residual lateral stress. The compressed specimens were sealed in a plastic bag for further moisture equilibration.

2.3. Test Procedures

2.3.1. Deformation Testing. Expansive deformation experiments were conducted to clear the factors which affected expansive strain. An oedometer frame is shown in Figure 5. The height of the specimen was 20.0 mm, and its cross-sectional area was 3000 mm^2. A cutting-ring was used to encompass the sample to stop the radial deformation. The vertical loading was loaded through the loading ram, which was connected to sample part and apparatus frame. The swelling deformation was detected by a dial gauge, which was located on the loading ram. The initial moisture contents of the specimen were 10.10, 12.85, 15.8, 18.3, and 22.19%. The designed dry densities were 0.14, 0.15, and 0.16 kN/m^3.

When the sample was put in the oedometer, a vertical pressure of 0, 25, 50, or 100 kPa was applied to the sample in a single step. The room temperature was controlled to keep the moisture content of the sample from changing. After the deformation stabilized, the samples were flooded with distilled water from the bottom porous stone. The water entered into the cell until 5 mm higher than the top surface of the sample. The swelling deformation was recorded every 2 hours. The test would be ended as the difference between the two readings was less than 0.01 mm. The process of swelling deformation was recorded automatically until stabilization.

2.3.2. Pressure Testing. Expansive stress experiment detected the expansive force in axial direction when the sample was fully saturated. Conventional oedometer was used to tests. Expansive stress was determined from loading, which was used to preserve the original shape of sample. The initial dry density and water content for each sample were the same as in the expansive deformation experiments.

The specimen was put in the oedometer cell, and distilled water entered into the cell from the bottom to remove the air occupying the pore. The sample was saturated from the bottom to the top of the sample. The displacement was recorded by the dial gauge as the sample was inundated, and the swelling of the sample was prevented by the application of loads. The load was applied by increasing the amount of sand, allowing an accurate measurement of the swelling pressure. Ideally, the dial gauge reading would not exceed 0.01 mm, to keep the sample from swelling and consolidation. The test was considered complete once the reading remained constant for at least two hours. Once the test was completed, the sample was removed, and the oven was used to determine the moisture content of the sample.

Figure 4: Sample after compaction.

Figure 5: Oedometer apparatus for the tests.

3. Results and Discussion

3.1. Results and Analysis of the Swelling Deformation Tests

3.1.1. Swelling Strain vs Time. Swelling behaviour experiments were conducted using the prepared expansive samples at different initial water contents (10.10, 12.85, 15.80, 18.30,

and 22.19%) and different dry densities (0.14, 0.15, and 0.16 kN/m^3). Figure 6 exhibited the swelling deformation developments with time. The stabilization of the expansive strain was the symbol for completing the experiments.

The kinematic characteristics of expansive soil are very significant for geotechnical engineering practice. There were three phrases for the swelling deformation time history on the basis of [21] and [22]. It is displayed in Figure 7.

According to swelling deformation time history in Figure 7, the second and third phase could be illustrated by the two coefficients of swelling. They are described in the following equations:

$$A_2 = \frac{\Delta L_2/L_0}{\Delta \lg T_2}, \qquad A_3 = \frac{\Delta L_3/L_0}{\Delta \lg T_3}, \tag{1}$$

where A_2 and A_3 are the swelling coefficients of the last two phases. ΔL_2 and ΔL_3 are the axial distortion through the second and third phases, respectively, and L_0 is the sample height at the beginning of the tests. $\Delta \lg T_2 = \lg T_{2e} - \lg T_{2s}$; $\Delta \lg T_3 = \lg T_{3e} - \lg T_{3s}$; the terminal and initial times during the second phase are T_{2e} and T_{2s}; the terminal and initial times during the third phase are T_{3e} and T_{3s}.

Table 1 shows the swelling coefficients for different initial water contents under the same dry density. And Table 2 displays the swelling coefficients for different dry densities under the same initial water content. It can be found from Table 1 that the swelling coefficient of the second phase (A_2) first increased and then decreased as the initial water content rose. The peak value of the swelling coefficient in the second phases was 0.56×10^{-1} while the moisture water content was 15.8%. When the moisture content was 22.19%, the minimum swelling coefficient was achieved. This result demonstrated that there was a threshold value of initial moisture content, above which primary expansion process would be depressed. According to Table 2, there was a negative correlation between swelling coefficient in the second phase and dry density. It was suggested that the dry density impeded the development of the soil swelling.

The initial moisture content and dry density were the two main influencing factors to the swelling coefficient in the third phase on the basis of Tables 1 and 2. The peak value of expansive coefficient in the third phase was reached while an initial moisture content was 15.8% based on Table 1. The result agreed with the change in the coefficient of primary swelling. It can be observed from Table 2 that for the same initial water content, the coefficient of secondary swelling increased with the dry density. Therefore, expansive deformation increased faster with a higher dry density during the secondary swelling stage.

3.1.2. Factors Influencing the Swelling Strain

(1) Dry Density Effect. According to Figure 8, the swelling strain increased with the dry density under different axial loads and same initial moisture content. The maximum value of axial deformation was 13.10% for the maximum dry density of 0.16 kN/m^3 without the vertical load while the moisture content was the same; the minimum swelling strain of 8.95% was observed while the dry density was 0.14 kN/m^3. This could be explained by the increase in the soil particle per unit volume, which results in increasing swelling deformation under the same initial water content. Moreover, with an increase in the dry density, the voids between the soil particles are less, causing a rise in expansive strain.

The expansive strain under 0 kPa was much greater than those for the samples under vertical stress but the same dry density. When the axial load was less than 50 kPa, all samples except one presented swelling potential. However, the samples collapsed as the axial pressure reached 100 kPa. The collapsibility became apparent when dry density was 0.14 kN/m^3. Meanwhile, swelling strain was also low, even though the dry density was 0.16 kN/m^3. Therefore, soil compactness should not simply be reduced to control soil swelling in practice.

The samples mainly showed expansibility under a small axial pressure. Collapse might occur with decreasing dry density. However, the samples mostly collapsed when the axial pressure became large. Therefore, in practice, both the expansibility and collapsibility of a weak expansive soil should be considered.

Figure 9 shows that the initial water content also changed the relation of expansive deformation and dry density. While initial moisture content was less than 18.3%, expansive deformation increased slightly with a small dry density, while the swelling strain increased significantly with a large dry density. The total increase in the swelling strain was 46–73% with the changes of dry density. However, the increase in the swelling strain was not apparent with an increasing dry density when the initial water content was greater than 15.8%, even as the dry density changed from 0.15 kN/m^3 to 0.16 kN/m^3. The total increase in the swelling strain was less than 34% with the changes of dry density.

(2) Initial Water Content Effect. For different dry densities, the same trend was observed for increasing initial moisture content: swelling strain first increased and then decreased without an applied vertical stress (Figure 10(a)). While the dry density was the minimum value, expansive strain increased from 8.95% to 10.667% and then decreased to 7.35% when the initial water content increased from 10.10% to 22.19%. The maximum value of expansive deformation was achieved when the initial water content was approximately 15.8% for all three different dry densities. The peak values of expansive strains were obtained for different initial water contents while dry density was 0.16 kN/m^3.

Nayak and Christensen [23], Çimen et al. [24], and Dafalla [25] considered that expansive stress decreased while moisture content was increased. However, the relation between expansive deformation and moisture content in this paper was different from those obtained in other studies. This difference can be explained as follows: under the same dry density, a sample with a smaller initial water content had more macropores (Tan et al. [26]). Therefore, the internal space was enough to allow soil swelling. As a result, the

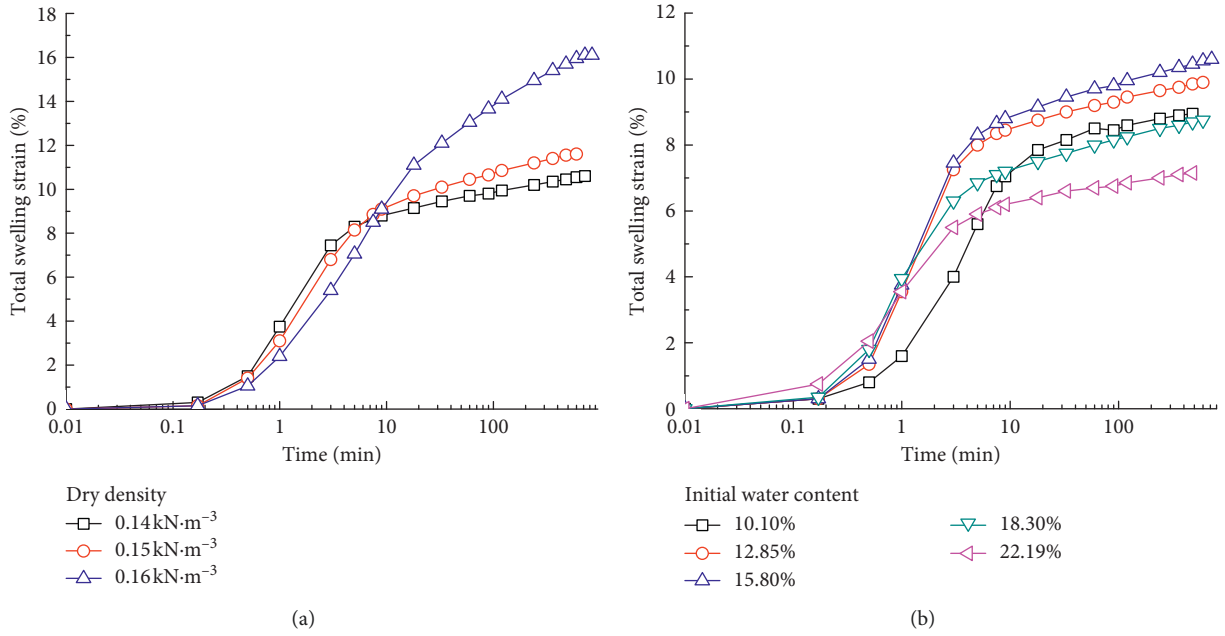

Figure 6: Relation of expansive deformation and log time. (a) Water content of 15.80%. (b) Dry density of 0.14 kN/m^3.

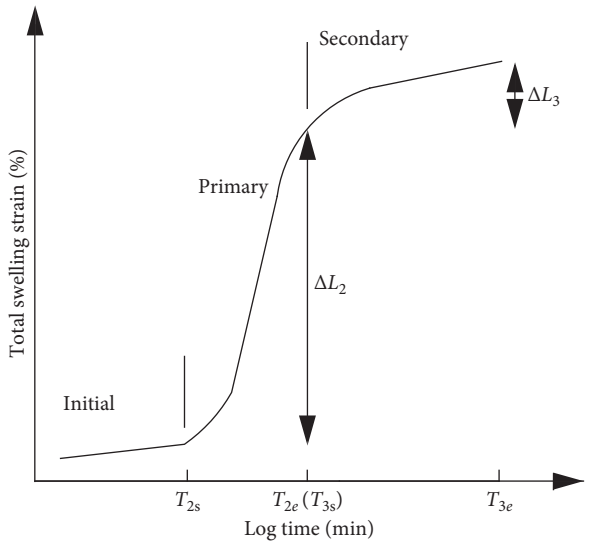

Figure 7: Three phases of swelling process.

Table 1: Coefficients of primary swelling and secondary swelling with dry density of 0.14 kN/m^3.

Moisture content (%)	A_2 (10^{-1})	A_3 (10^{-2})
10.10	0.39	0.93
12.85	0.54	0.98
15.80	0.56	1.13
18.30	0.46	1.01
22.19	0.36	0.67

Table 2: Coefficients of primary swelling and secondary swelling for an initial moisture content of 15.8%.

Dry density (kN/m^3)	A_2 (10^{-1})	A_3 (10^{-2})
0.14	0.56	1.13
0.15	0.53	1.47
0.16	0.53	2.90

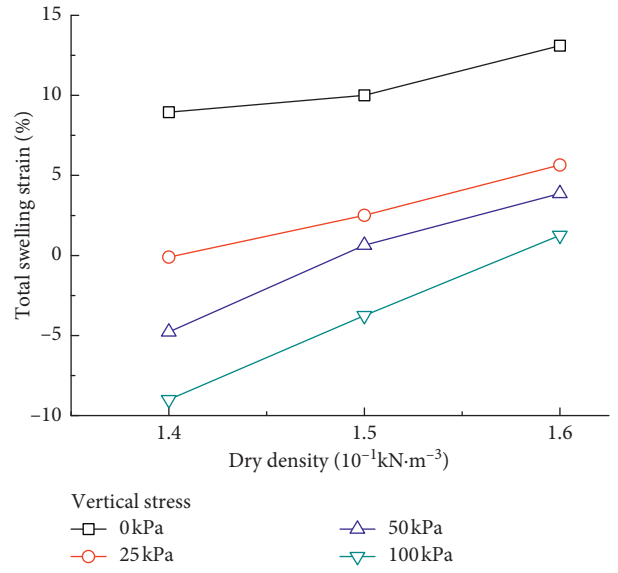

Figure 8: Relation between the swelling strain and dry density for the moisture content of 10.10%.

measured expansion strain energy and the swelling strain were small. With an increase in the initial water content, the proportion of macropores decreased. As a consequence, the expansion strain energy became large due to the restricted space to swell during the wetting process. Consequently, the measured swelling strain increased. Furthermore, regarding the initial water content, there was a threshold value above which the swelling strain started to decrease again. The

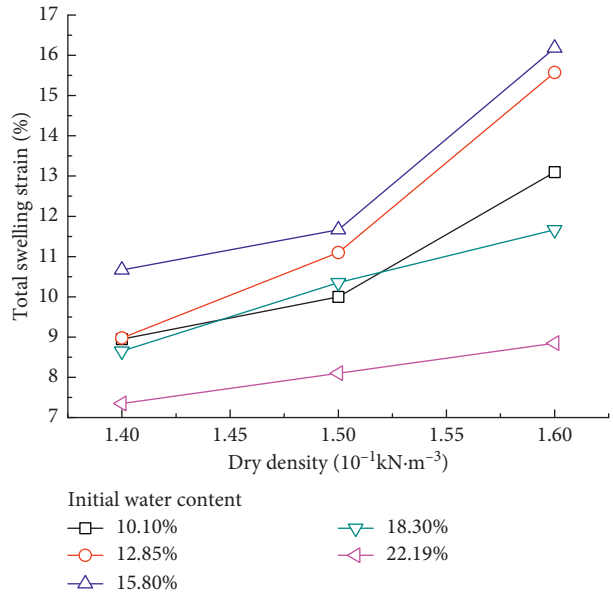

Figure 9: Relation of expansive deformation and dry density without a vertical load.

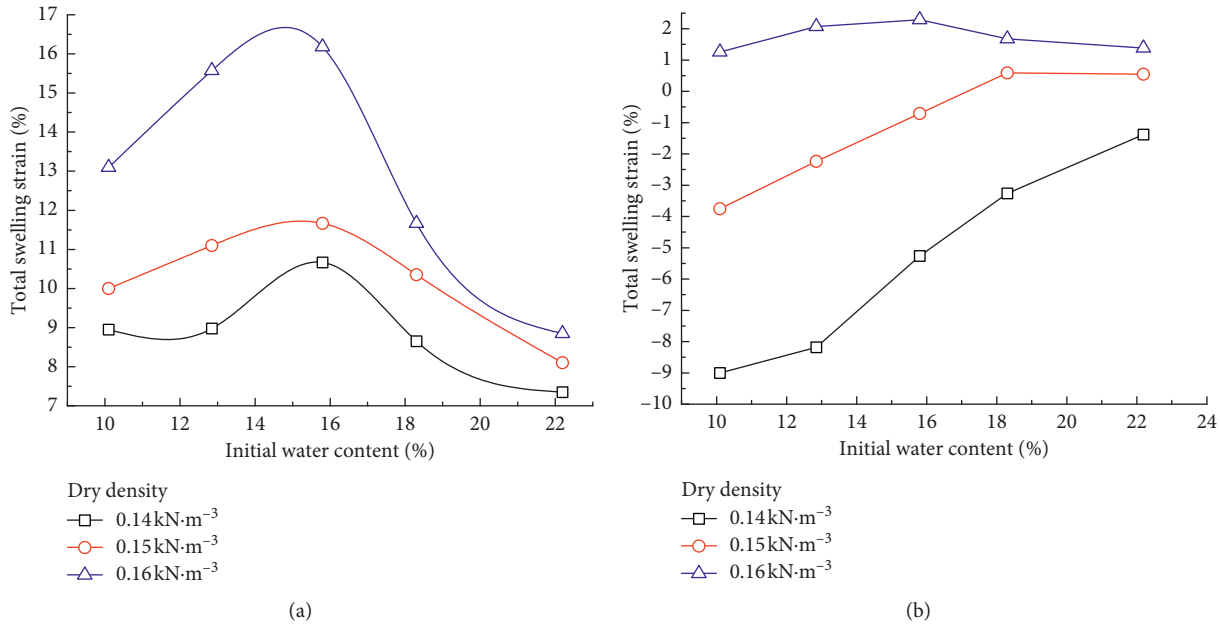

Figure 10: Relation of expansive strain and moisture content for diverse axial pressure. (a) Axial pressure of 0 kPa. (b) Axial pressure of 100 kPa.

reason for this decrease in swelling strain was that the swelling deformation developed more with higher initial water contents during the process of sampling; therefore, the expansion strain energy became small during the swelling tests. Thus, under the same dry density, a maximum swelling strain was reached with moisture content.

Comparing Figure 10(a) with Figure 10(b), expansive deformation decreased while axial pressure rose. When the vertical stress was 100 kPa, the swelling strain was less than zero while dry densities were 0.14 kN/m^3 and 0.15 kN/m^3. Therefore, samples collapsed in the course of wetting process. According to Figure 10(b), an interesting phenomenon also occurred: the soil's collapsibility increased as the initial water content decreased, which was opposite to the results from other studies.

Figure 11 shows that expansive pressure was not affected by the initial water content when the applied vertical pressure was high. Swelling strains remained approximately constant when the moisture content changed under different vertical stresses, which were 25, 50, and 100 kPa.

(3) Axial Pressure Effect. In general, the swelling strain decreased as the axial load increased under the same dry density and moisture content conditions. Figure 12 displays that expansive strain decreased sharply as the axial pressure increased from 0 kPa to 25 kPa, while it tended to decrease

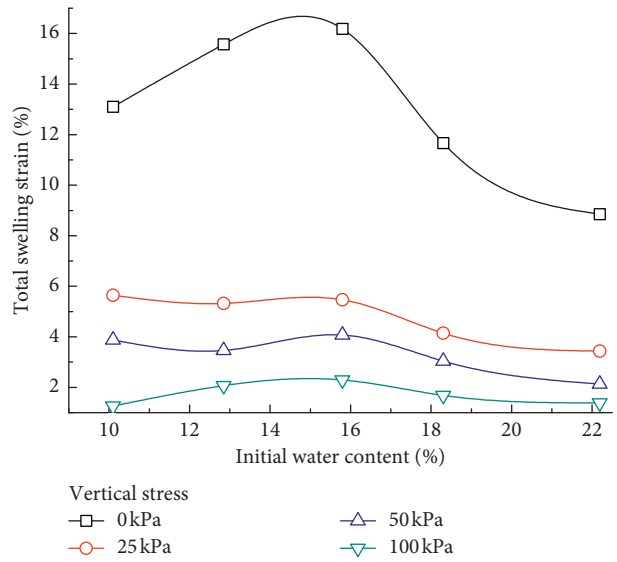

Figure 11: Relation between the swelling strain and moisture content with dry density of 0.16 kN/m^3.

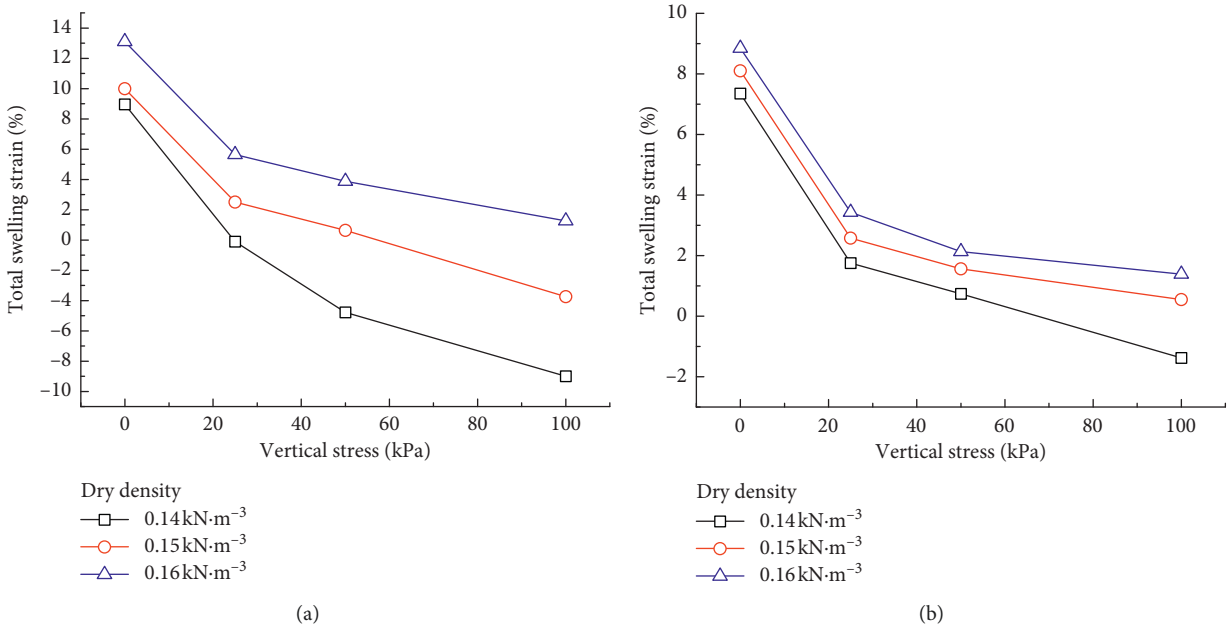

Figure 12: Relation between the swelling strain and vertical stress for different initial water contents. (a) Initial water content of 10.10%. (b) Initial water content of 22.19%.

slowly as the vertical pressure increased from 25 kPa to 100 kPa. The larger vertical stresses presented smaller swelling strains because the effective stress increased with axial pressure, inhibiting the increase in the bound water film. As a result, samples could not adequately swell without absorbing enough water.

Under the same vertical stress and moisture content, expansive strain rose with dry density. Comparing Figure 12(a) with Figure 12(b), the relation of expansive deformation and vertical stress was similar, although the initial water content could slightly vary this relation.

Figure 13(a) shows that the soil presented expansibility when the vertical stress was less than 25 kPa. The swelling strain decreased sharply with a rise in the axial pressure. However, when the applied vertical load was greater than 50 kPa, the samples collapsed during wetting at a dry density of 0.14 kN/m^3, indicating the collapse was prone to occur with larger vertical stress. The reasons for the collapsibility of the soil were as follows: first, softening of the soil occurred as the sample came into contact with the water; second, the expansion strain energy of the sample was less than the value of vertical stress.

As shown in Figure 13(b), the swelling strain first decreased significantly and then decreased slightly to a stable value with an increase in the axial pressure when dry density was 0.16 kN/m^3. All of the samples expanded under any

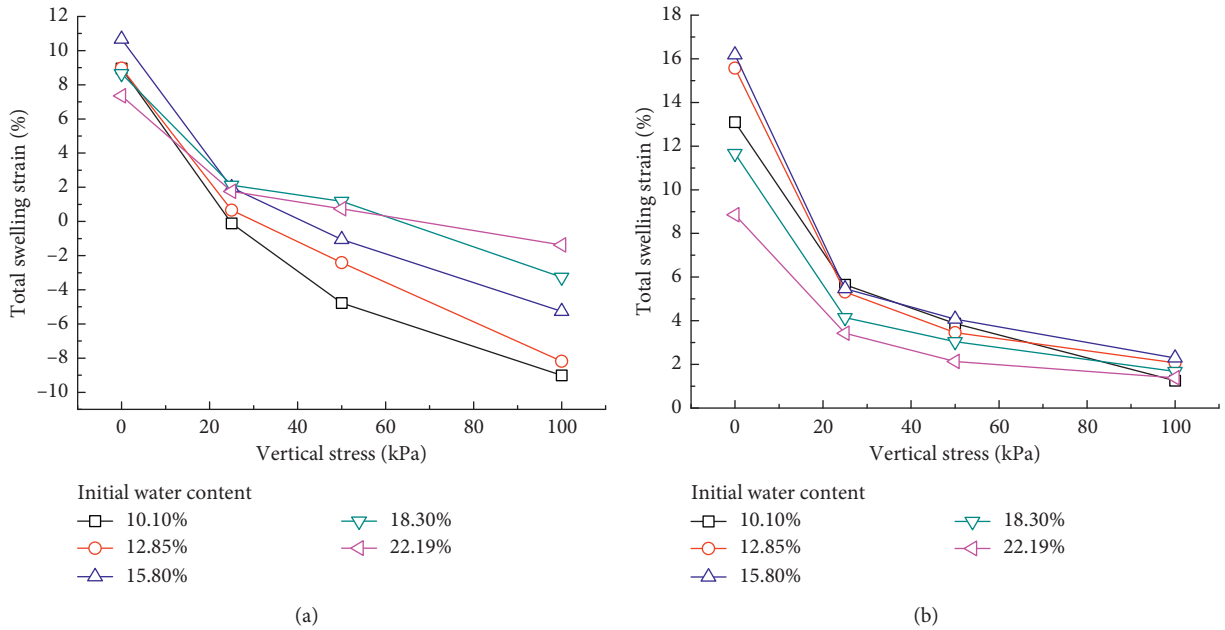

Figure 13: Relation of expansive deformation and axial stress for different dry densities. (a) Dry density of 0.14 kN/m^3. (b) Dry density of 0.16 kN/m^3.

vertical load. Therefore, with high compaction, the sample was expandable even though the sample was under a heavy applied vertical load.

3.1.3. Compression Characteristics. Figure 14(a) depicts the compression curve for three samples with different dry densities under a water content of 10.10%. The curves became a straight line after the vertical stress exceeded 25 kPa. Compression index was calculated according to the slope of the straight line. The calculated compression indexes are shown in Table 3. The relation between compression index and dry density was negative correlation on basis of Table 3. Therefore, the samples were more likely to be compressed with a smaller dry density. There was a consistent law for initial water content of 15.8%, as shown in Figure 14(b).

Generally, soil compressibility is related to the moisture content. However, in the research, soil compressibility first increased and then decreased with a rise in moisture content in Figure 15. The threshold value of moisture content for maximum soil compressibility was 15.8%. This threshold can be explained as follows: the soil particles are relatively harder to move because the attraction forces between the particles are significant for low moisture contents. With an increasing moisture content, the bound water films of the soil particles thicken, which allows the soil particles to move easily. Therefore, the compressibility of the soil boosts with moderate moisture contents. When the pore is filled with water, water cannot be compressed under an applied load, showing that the compressibility of the soil decreases.

3.2. Results and Analysis of the Swelling Pressure Tests

3.2.1. Swelling Pressure vs Time. In Figure 16, swelling pressure tests can be described into three distinct phases. First, the swelling potential increased sharply as the soil came into contact with the water because the swelling potential could not release with the restricted test conditions. The swelling pressure increased linearly at this stage. Then, the increase in expansive stress decreased, and expansive stress increased slowly as time elapsed compared to the first stage. Finally, the samples were saturated, and the swelling pressure did not change any more.

The ultimate expansive stress increased with dry density under same moisture content. Figure 16(a) shows that the maximum swelling pressure occurred when the dry density was 0.16 kN/m^3. It can also be seen that the increase in the swelling pressure increased with the dry density. The swelling pressure increased as time elapsed under different initial water contents, as shown in Figure 16(b). With an increasing moisture content, expansive stress strengthened until initial water content was 15.8%. Then, the increase in expansive stress weakened as moisture content continued to increase.

3.2.2. Factors Influencing the Swelling Pressure

(1) Dry Density Effect. Expansive stress clearly rose with dry density based on Figure 17. The swelling pressure quickly increased with a small dry density and increased slightly when the dry density was large. For example, the swelling pressure changed from 46.28 kPa to 120.10 kPa with an increase in small dry density at a water content of 12.85%. However, the swelling pressure increased from 120.10 kPa to 293.54 kPa with an increase in large dry density. It was concluded that the dry density effect was considerable when the dry density was greater than 0.15 kN/m^3, which is useful reference for geotechnical engineering applications.

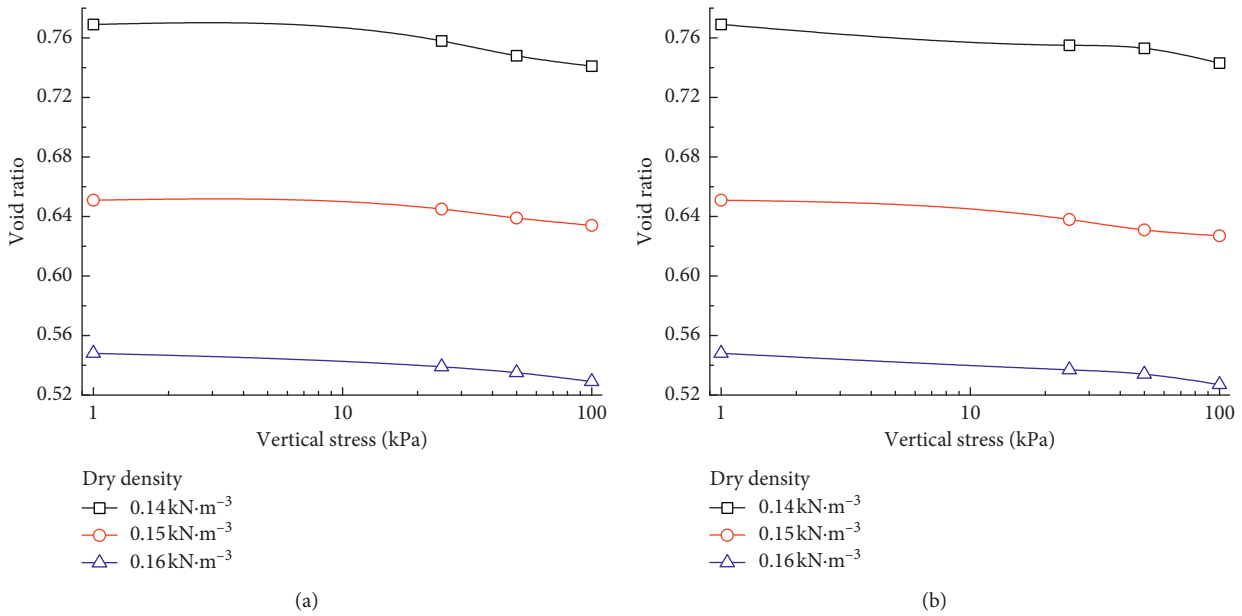

Figure 14: Relation between axial pressure and void ratio for different initial water contents. (a) Initial water content of 10.10%. (b) Initial water content of 15.8%.

Table 3: Compression index of the samples.

Water content (%)	Dry density (kN/m^3)	Compression index
10.10	0.14	0.028
	0.15	0.018
	0.16	0.016
15.80	0.14	0.019
	0.15	0.018
	0.16	0.016

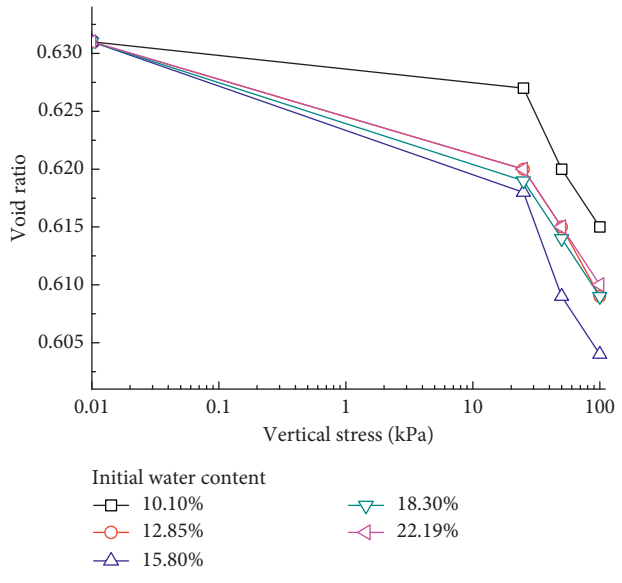

Figure 15: Relation between axial pressure and void ratio for dry density of 0.15 kN/m^3.

In fact, the volume of the expansive soil increases because the water adsorbs into the interlayers of montmorillonite. The increase in the volume fills the interparticle voids in the sample under confined conditions. The swelling pressure increases as the voids are filled. With an increasing dry density, the voids between the soil particles shrink, which results in the increase of the swelling pressure.

Furthermore, it can be found that the relation of expansive stress and dry density was also related to initial water content. Specifically, when the initial water content was 10.10%, the swelling pressure increased by 170.03 kPa with the increase of dry density. The corresponding values were 254 kPa and 86.85 kPa when moisture contents were 15.8% and 22.19%. Therefore, the maximum increase in expansive stress occurred with the increase of dry density under moisture content of 15.8%.

The relationship of swelling pressure and dry density could be described by the power function. The fitted function could be described as follows:

$$Q = a * \rho_d^b, \tag{2}$$

where ρ_d stands for dry density and Q represents expansive stress. a and b represent coefficients for different water contents. The related parameters were calculated and are listed in Table 4.

(2) Moisture Content Effect. Figure 18 shows that the swelling pressure initially increased and then reduced with an increasing moisture content under three dry densities tested. When dry densities were small, for example, 0.14 kN/m^3 or 0.15 kN/m^3, swelling pressure was smaller than a sample with larger dry density. Therefore, the dry density had a greater impact on expansive pressure than the moisture content. Specifically, for moisture content of 10.10%, the swelling pressures were 29.92 kPa and 85.03 kPa while the dry densities were 0.14 kN/m^3 and 0.15 kN/m^3, respectively. However, swelling pressure was 199.95 kPa for a dry density

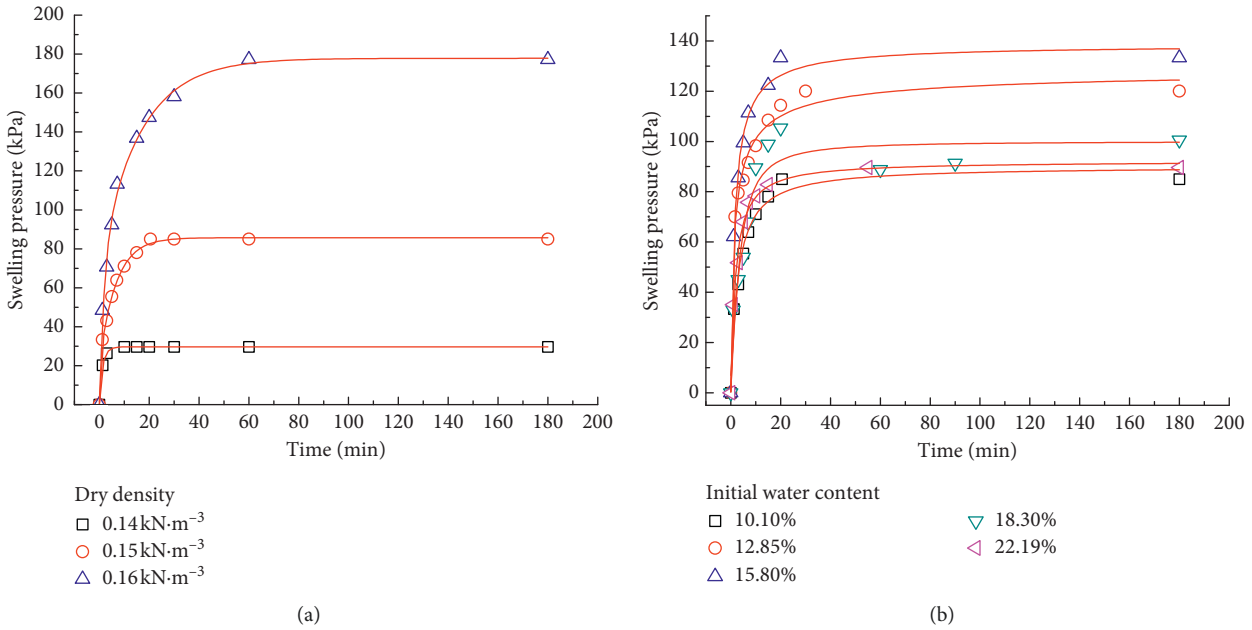

Figure 16: Relation between the swelling pressure and time. (a) Initial water content of 10.10%. (b) Dry density of 0.15 kN/m^3.

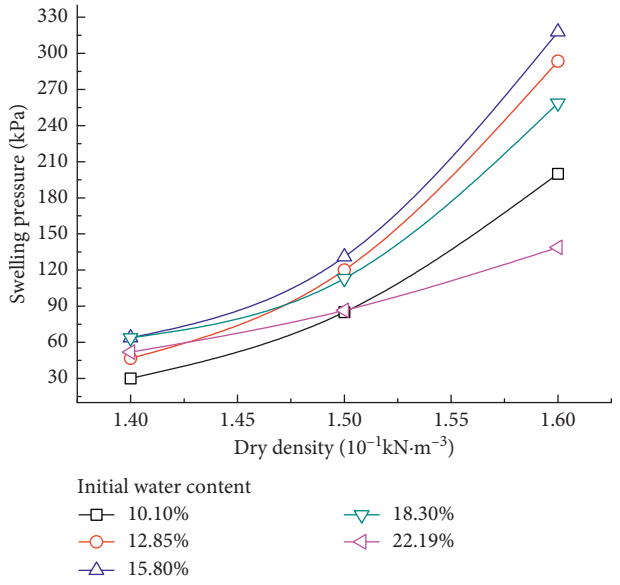

Figure 17: Relation of expansive stress and dry density with different initial water contents.

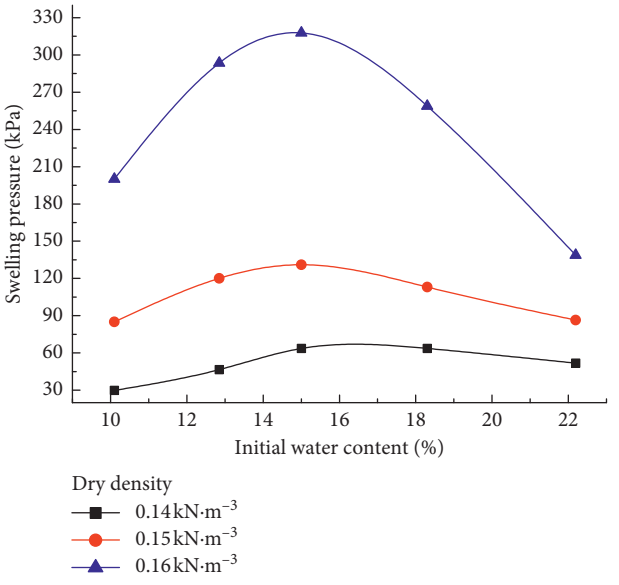

Figure 18: Relationship between expansive stress and moisture content for diverse dry densities.

Table 4: Fitting equations for the relationship of expansive stress and dry density.

Initial water content (%)	Equation	Coefficient of correlation R^2
10.10	$Q = 0.32802 * \rho_d^{13.64854}$	0.99864
12.85	$Q = 0.44429 * \rho_d^{13.81507}$	0.99999
15.80	$Q = 0.72501 * \rho_d^{12.93214}$	0.9944
18.30	$Q = 1.10669 * \rho_d^{11.588}$	0.9848
22.19	$Q = 4.38602 * \rho_d^{7.35002}$	0.99998

of 0.16 kN/m^3, which was 6.68 and 2.35 times the corresponding values of the dry densities of 0.14 kN/m^3 and 0.15 kN/m^3.

Jayalath et al. [20], Çimen et al. [24], and Dafalla [25] considered expansive stress decreased monotonically with a rise in the moisture content. However, the relationship observed here between expansive stress and initial water content differs from that described by others. This difference could be explained as follows: under the same dry density, a sample with a smaller initial water content had more macropores (Tan et al. [26]). A sufficient volume of internal pore space reduced soil swelling. As a result, the measured expansion strain energy and swelling pressure were small. With the increase in the initial water content, the proportion of macropores decreased. As a consequence, the expansion strain energy increased due to the restriction of space during

the wetting process. Therefore, the measured swelling pressure increased. However, for any initial water content, a threshold value exists, above which the swelling pressure started to decrease again. Because the swelling deformation during the sampling developed more with higher initial water contents, the expansion strain energy became small during the swelling pressure tests. Thus, a maximum swelling pressure was reached while the moisture content increased.

The relation of expansive stress and moisture content was in accordance with the relation of expansive deformation and water content achieved from expansive deformation tests. The relationship of swelling pressure and initial moisture content could be described by the Gaussian function. The function expression was described as follows:

$$Q = y_0 + \frac{A}{w\sqrt{\pi/2}} e^{-2\left((w_0 - x_c)^2/w^2\right)}, \quad (3)$$

where w_0 is the initial water content and y_0, A, w, and x_c are the parameters for different dry densities. The related parameters are shown in Table 5.

3.3. Comparison of the Results from Expansive Deformation and Expansive Pressure Tests

3.3.1. Stress Path Effects. Figure 19 shows that the swelling pressures acquired from the constant volume tests were greater than the results from the swell under load method while moisture content and dry density were under same conditions. Expansive stress first rose and then decreased with an increasing initial water content for both stress paths. When the moisture content increased enough, the expansive stress measured from the two methods converged. As a result, the stress path effect was minimized.

Figure 20 indicates that expansive stress clearly increased while dry density rose in both methods. Difference in expansive stress resulted from two stress paths increased while the dry density rose.

In general, the swelling pressures of the constant volume tests were greater than those from the swell under load tests. The above results could be explained as follows. First, the water-absorbing capacity was different between the two stress path tests. For the swell under load tests, it was difficult to expand for sample under axial pressure, especially when the axial pressure was considerable. Second, the friction between particles was different between the two stress tests. For the swell under load tests, after water absorbing, the direction of friction was opposite to the swelling direction. However, the direction of friction was first opposite to the swelling direction and then along the swelling direction as the axial pressure increased, balancing the swelling pressure for the constant volume tests. Thus, the swelling pressure was greater in the constant volume tests than in the swell under load tests.

3.3.2. Relationship of Expansive Stress and Expansive Strain. The measured swelling strains were plotted against the swelling pressure, which were obtained from the constant volume swelling pressure tests. As shown in Figure 21, there was a unique relationship of expansive deformation and expansive stress, represented by the following equation:

Table 5: Fitting equations for relation of expansive pressure and water content.

ρ_d (kN/m^3)	Equation	Coefficient of correlation R^2
0.14	$Q = -7.57537 + 72.81553e^{-((w_0 - 17.85401)^2/90.13477)}$	0.96877
0.15	$Q = 79.86626 + 53.60285e^{-((w_0 - 15.40976)^2/17.07494)}$	0.87335
0.16	$Q = 88.91567 + 234.36418e^{-((w_0 - 15.02841)^2/32.98019)}$	0.99878

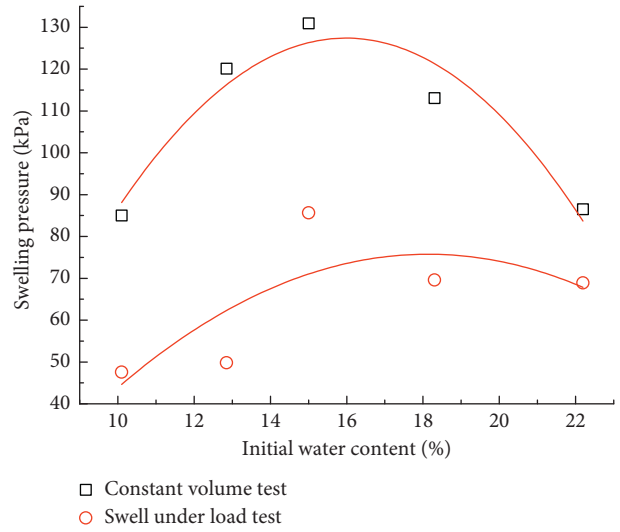

Figure 19: Relation between expansive stress and initial water content for two diverse stress paths.

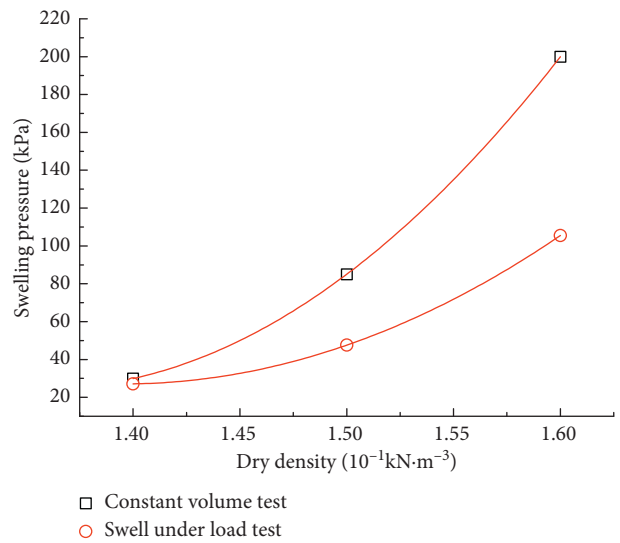

Figure 20: Relationship of expansive stress and dry density with same water content of 10.10% for two stress path tests.

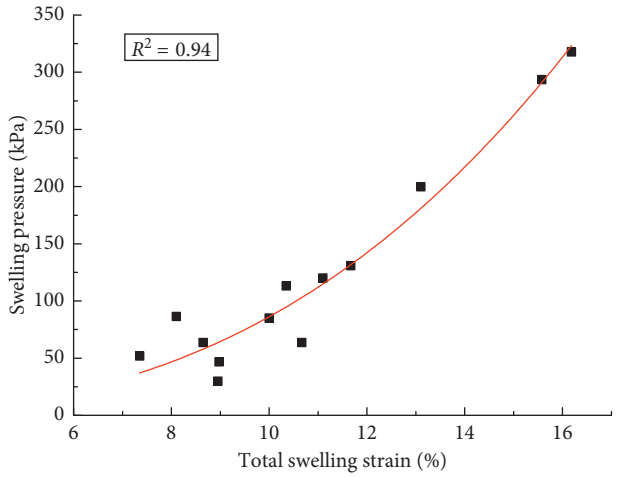

Figure 21: Relation of expansive stress and expansive strain.

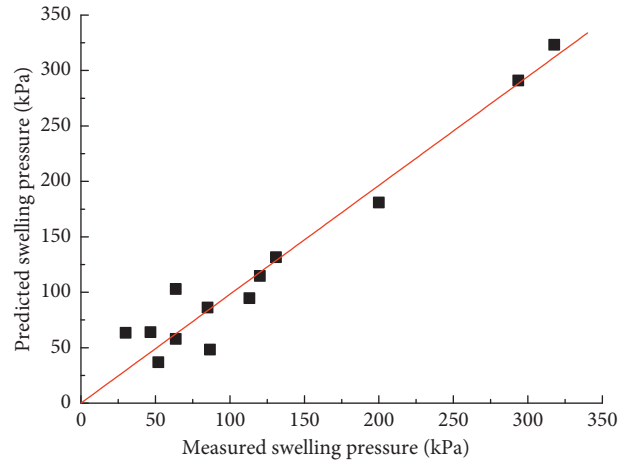

Figure 22: Relationship of measured expansive stress and expansive stress predicted by this study.

$$Q = 0.1548 * S^{2.7455}, \quad R^2 = 0.94, \tag{4}$$

where S is the swelling strain. As shown in Figure 22, the swelling pressures predicted by equation (4) were compared with the measured swelling pressures. The coefficient of correlation between the predicted and measured data was 0.97, which confirmed the existing strong correlation between the swelling pressure and swelling strain. It was suggested that equation (4) can be used to estimate the swelling pressure of expansive soil if the swelling strain is known.

4. Conclusion

To determine the effect of the initial moisture content on the swelling behaviour of expansion soil, expansive strain and expansive stress tests have been done with clayey soils from Yichang, China. Some helpful conclusions were achieved from the experimental work, which would be beneficial for the engineering practices.

(1) The relation between the swelling pressure and initial moisture content was not monotonic. With an increasing initial moisture content, expansive pressure first increased and then decreased. These results could be explained by the change in the microstructure as the water content increased; this relationship could be described by a Gaussian function. The coefficient of correlation was 0.99 for the dry density of 0.16 kN/m^3, suggesting a good fit between expansive stress and moisture content using the Gaussian distribution. The relationship of expansive stress and dry density could be fitted well by a power function.

(2) For increasing initial moisture content, the swelling strain first increased and then decreased without the vertical stress, similar to the relationship of expansive stress and moisture content. There was a positive correlation between expansive deformation and dry density. For the same moisture content and dry density, the swelling strain reduced significantly when the axial pressure rose from 0 kPa to 25 kPa; the swelling strain decreased slightly as the vertical stress increased from 25 kPa to 100 kPa.

(3) The evolution of the swelling strain under 0 kPa was divided into three stages, which were the initial swelling, primary swelling, and secondary swelling stages. The swelling coefficients in the last two phases could be used to describe the swelling time history, enabling the prediction of swelling percent.

(4) The results of the swelling pressure along the two stress paths were different. Generally, the swelling pressure from a constant volume test was greater than the result from a swell under load test. A monotonous relation between the swelling pressure and swelling strain was achieved, as expressed by equation (4). This equation could be used to calculate the one parameter, if the other parameter was known.

Data Availability

The data used to support the findings of this study are available from the corresponding author upon request.

Conflicts of Interest

The authors declare that there are no conflicts of interest regarding the publication of this paper.

Acknowledgments

This research was funded by the specialized research fund for the doctoral program of China (grant no. 20120162110023).

References

[1] A. Sridharan and M. S. Jayadeva, "Double layer theory and compressibility of clays," *Géotechnique*, vol. 32, no. 2, pp. 133–144, 1982.

[2] S. Tripathy, A. Sridharan, and T. Schanz, "Swelling pressures of compacted bentonites from diffuse double layer theory," *Canadian Geotechnical Journal*, vol. 41, no. 3, pp. 437–450, 2004.

[3] T. V. Bharat, P. V. Sivapullaiah, and M. M. Allam, "Novel procedure for the estimation of swelling pressures of compacted bentonites based on diffuse double layer theory," *Environmental Earth Sciences*, vol. 70, no. 1, pp. 303–314, 2012.

[4] T. Schanz, M. I. Khan, and Y. Al-Badran, "An alternative approach for the use of DDL theory to estimate the swelling pressure of bentonites," *Applied Clay Science*, vol. 83-84, pp. 383–390, 2013.

[5] W. K. Wray, B. M. El-Garhy, and A. A. Youssef, "Three-dimensional model for moisture and volume changes prediction in expansive soils," *Journal of Geotechnical and Geoenvironmental Engineering*, vol. 131, no. 3, pp. 311–324, 2005.

[6] H. H. Adem and S. K. Vanapalli, "Constitutive modeling approach for estimating1-Dheave with respect to time for expansive soils," *International Journal of Geotechnical Engineering*, vol. 7, no. 2, pp. 199–204, 2013.

[7] B. Lin and A. B. Cerato, "Prediction of expansive soil swelling based on four micro-scale properties," *Bulletin of Engineering Geology and the Environment*, vol. 71, no. 1, pp. 71–78, 2011.

[8] S. S. Agus, Y. F. Arifin, S. Tripathy, and T. Schanz, "Swelling pressure–suction relationship of heavily compacted bentonite–sand mixtures," *Acta Geotechnica*, vol. 8, no. 2, pp. 155–165, 2012.

[9] Q. Wang, Y.-J. Cui, A. M. Tang, P. Delage, B. Gatmiri, and W.-M. Ye, "Long-term effect of water chemistry on the swelling pressure of a bentonite-based material," *Applied Clay Science*, vol. 87, no. 1, pp. 157–162, 2014.

[10] Y.-G. Chen, C.-M. Zhu, W.-M. Ye, Y.-J. Cui, and B. Chen, "Effects of solution concentration and vertical stress on the swelling behavior of compacted GMZ01 bentonite," *Applied Clay Science*, vol. 124-125, pp. 11–20, 2016.

[11] G. Sarkar and S. Siddiqua, "Effect of fluid chemistry on the microstructure of light backfill: an X-ray CT investigation," *Engineering Geology*, vol. 202, pp. 153–162, 2016.

[12] S. Saba, J.-D. Barnichon, Y.-J. Cui, A. M. Tang, and P. Delage, "Microstructure and anisotropic swelling behaviour of compacted bentonite/sand mixture," *Journal of Rock Mechanics and Geotechnical Engineering*, vol. 6, no. 2, pp. 126–132, 2014.

[13] T. Schanz and Y. Al-Badran, "Swelling pressure characteristics of compacted Chinese Gaomiaozi bentonite GMZ01," *Soils and Foundations*, vol. 54, no. 4, pp. 748–759, 2014.

[14] Y. Erzin and N. Gunes, "The unique relationship between swell percent and swell pressure of compacted clays," *Bulletin of Engineering Geology and the Environment*, vol. 72, no. 1, pp. 71–80, 2013.

[15] J.-L. Briaud, X. Zhang, and S. Moon, "Shrink test-water content method for shrink and swell predictions," *Journal of Geotechnical and Geoenvironmental Engineering*, vol. 129, no. 7, pp. 590–600, 2003.

[16] D. D. Overton, K. C. Chao, and J. D. Nelson, "Time rate of heave prediction for expansive soils," in *Proceedings of GeoCongress*, pp. 1–6, Atlanta, GA, USA, February 2006.

[17] S. Kaufhold, W. Baille, T. Schanz, and R. Dohrmann, "About differences of swelling pressure—dry density relations of compacted bentonites," *Applied Clay Science*, vol. 107, pp. 52–61, 2015.

[18] V. Sivakumar, J. Zaini, D. Gallipoli, and B. Solan, "Wetting of compacted clays under laterally restrained conditions: initial state, overburden pressure and mineralogy," *Géotechnique*, vol. 65, no. 2, pp. 111–125, 2015.

[19] M. V. Villar and A. Lloret, "Influence of dry density and water content on the swelling of a compacted bentonite," *Applied Clay Science*, vol. 39, no. 1, pp. 38–49, 2008.

[20] C. P. G. Jayalath, C. Gallage, and N. S. Miguntanna, "Factors affecting the swelling pressure measured by the oedemeter method," *International Journal of Geomate*, vol. 11, no. 24, pp. 2397–2402, 2016.

[21] A. Sridharan and Y. Gurtug, "Swelling behaviour of compacted fine-grained soils," *Engineering Geology*, vol. 72, no. 1-2, pp. 9–18, 2004.

[22] S. M. Rao and T. Thyagaraj, "Role of direction of salt migration on the swelling behaviour of compacted clays," *Applied Clay Science*, vol. 38, no. 1-2, pp. 113–129, 2007.

[23] N. V. Nayak and R. W. Christensen, "Swelling characteristics of compacted expansive soils," *Clays and Clay Minerals*, vol. 19, no. 4, pp. 251–261, 1974.

[24] Ö. Çimen, S. N. Keskin, and H. Yıldırım, "Prediction of swelling potential and pressure in compacted clay," *Arabian Journal for Science and Engineering*, vol. 37, no. 6, pp. 1535–1546, 2012.

[25] M. A. Dafalla, "The influence of placement conditions on the swelling of variable clays," *Geotechnical and Geological Engineering*, vol. 30, no. 6, pp. 1311–1321, 2012.

[26] Y. Z. Tan, X. J. Hu, and B. Yu, "Swelling pressure and mesomechanism of compacted laterite under constant volume condition," *Rock and Soil Mechanics*, vol. 35, no. 3, pp. 653–658, 2014.